

1  
COMMISSARIAT A L'ENERGIE ATOMIQUE

FR 8803500

CENTRE D'ETUDES NUCLEAIRES DE SACLAY

CEA-CONF --9295

Service de Documentation

F91191 GIF SUR YVETTE CEDEX

MI  
102

METRICH N. - MOSBAH M. - TROCELLIER P. - CLOCCHIATTI R.

CEA Centre d'Etudes Nucléaires de Saclay, 91 - Gif-sur-Yvette (FR).  
Dept. de Physico-Chimie

NUCLEAR MICROPROBE ANALYSIS OF CARBON WITHIN GLASS  
INCLUSIONS AND VOLCANIC MATERIALS

Communication présentée à : 11. International congress on X-ray optics and  
microanalysis

London, ON (CA)  
4-8 Aug 1986

# NUCLEAR MICROPROBE ANALYSIS OF CARBON WITHIN GLASS INCLUSIONS AND VOLCANIC MATERIALS

N. METRICH, M. MOSBAH, P. TROCELLIER, R. CLOCCHIATTI  
Centre d'Etudes Nucleaires de Saclay, France

Elements such as C, H, N, S, Cl represent the major components of the volatile phase dissolved in magmas. These dissolved gases could be preserved within glasses (or silicate melt inclusions) trapped during crystal growth.

Microanalysis possibilities have been explored to determine light element concentrations within glasses (melt inclusions and basaltic glass fragments) and volcanic phenocrysts. In the first step, C was examined. The study of different spectral interferences lead to calculated detection limits of 40  $\mu\text{g/g}$  for basaltic glasses and 50  $\mu\text{g/g}$  for olivine crystals. The C contents of all investigated specimens range from 40  $\mu\text{g/g}$  (the detection limit) to 6800  $\mu\text{g/g}$ . Heterogeneities were revealed within glass inclusions. Measurements show obvious concentration profiles in basaltic glass samples. Our results agree with previous published data and are reliable. Accuracy of measurements is about 20%.

## Selected Samples

Basaltic glass fragments were examined to specify the analysis conditions and to determine detection limits. The specimen ALV 981 R23 was collected by the Alvine submersible at -2600 meters, in the east part of Pacific rise (Gulf of California) (1)

Melt inclusions: the measurements were carried out on a first population of glasses trapped within olivine crystals (Fo 82) from Mount Etna scoriae (Italy). Glass compositions are hawaiitic ( $\text{MgO}=5.5 \text{ wt}\%$ ,  $\text{K}_2\text{O}/\text{Na}_2\text{O}=0.5$ ) (2). The other specimens come from Piton de la Fournaise Volcao (Reunion), for which basaltic melts were included in olivine Fo 84 (3). Investigated melt inclusions (except Mt. Rossi sample (4)) contain both a glass phase and a shrinkage bubble (appeared during the cooling). Their sizes vary from 80 to 250  $\mu\text{m}$ .

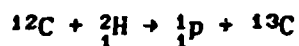
Minerals: olivine and scapolite were studied. The olivine crystals are those of the Etnean scoriae and of the Reunion lavas. Other olivine samples come from San Carlos (Arizona) (4-6). The scapolite crystals originate from Chuquet-Genestoux (Chaine des Puys, France). It is likely that they have crystallized under high pressure conditions (greater than 10 Kb) (7).

## Preparation

The samples were polished using  $\text{Al}_2\text{O}_3$  paste, to 0.3  $\mu\text{m}$  in grain size. Then, they were washed in bi-distilled water using an ultrasonic cleaner. The smallest specimens were embedded in a resin. A thin gold surface coating was used to prevent charging.

### Experimental Conditions

Samples are bombarded under vacuum with a deuteron microbeam ( $E_d=1.45$  MeV; current = 500 pA; spot diameter=5-10  $\mu\text{m}$ )(8). The following non resonant reaction is used:



The charged particles (protons) emitted consecutively to these nuclear interactions are detected by means of an annular surface barrier detector. A mylar foil (thickness: 25  $\mu\text{m}$ ) to absorb the elastically backscattered deuterons, is placed in front of the detector. The observation angle ranges from  $120^\circ$  to  $180^\circ$  with respect to incident beam direction. The protons released from reaction 1 have a maximum energy  $E_p=3.26$  MeV, the detected energy after the mylar foil is around 2.80 MeV.

### Analysis Progress

First, the existence of some parasitic effects which can distort the measurements should be noted. They have two origins: the C surface contamination and the nuclear interferences with the different matrix components. The first can be solved by preparing a thin C film (~16 nm) coated on a natural glass sample which will be analyzed under the same conditions. Thus, the C surface region contribution to the experimental spectrum is defined and can be subtracted for further content calculations. The major glass and mineral components are light elements as Si (~45 wt%), Al (~20 wt%) and Mg (~8 wt%). Each of them gives a charged particle spectrum with peaks contributing to the carbon analysis background. Interference ratios can be calculated and then subtracted from the C contribution to perform more accurate determinations.

A graphite sample with a known density is used as standard (figure 1)

Table 1 Carbon contents in different samples

Sample	Glass ( $\mu\text{g/g}$ )	Mineral ( $\mu\text{g/g}$ )
ALV 981 R23	1500 $\pm$ 400 $\rightarrow$ 100 $\pm$ 30	
Scapolite Boivin		6800 $\pm$ 1100
San Carlos Olivine		250 $\pm$ 60 $\rightarrow$ 100 $\pm$ 30
Piton de la Fournaise	{detection limit (= 60 $\mu\text{g/g}$ )	{detection limit
ETNA Silvestri (1) (1892)	500 $\pm$ 100	{detection limit
Silvestri (2) (1892)	70 $\pm$ 20	idem
Mt. Rossi (1) (1669)	600 $\pm$ 150	{detection limit
Mt. Rossi (2) (1669)	120 $\pm$ 30	idem

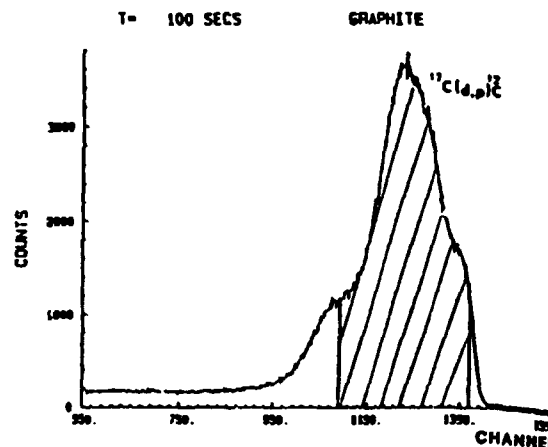
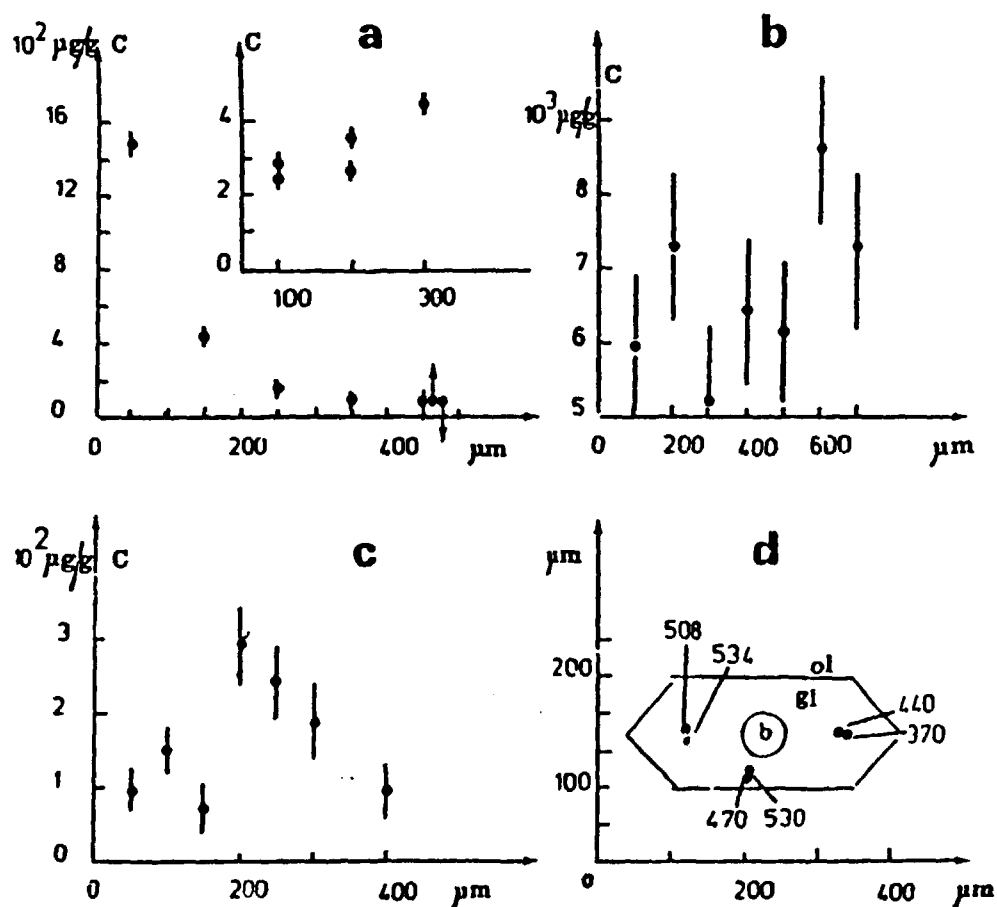
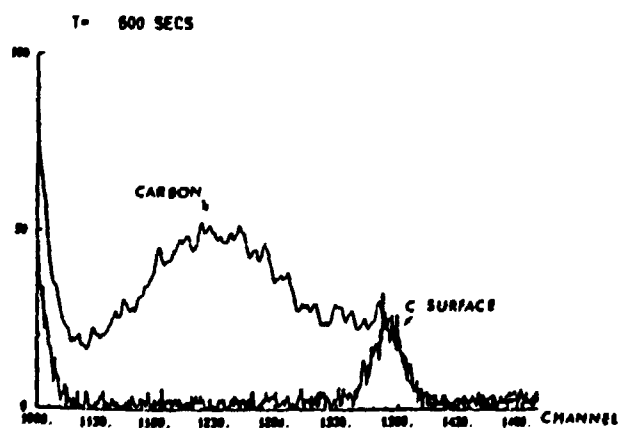


Figure 1. Charged particle spectrum from graphite sample ( $E_d=1.45$  MeV; current=300-500 pA; counting time = 100 s; beam size=50  $\mu\text{m}^2$ ). The cross hatched zone corresponds to that considered for content calculation.



**Figure 2.** (a) Carbon content variations in ALV 981 R23 glass sample along two horizontal lines as a function of distance. Arrows indicate 100  $\mu\text{m}$  vertical displacement. (b) Carbon distribution within scapolite from "Chaîne des Puys". The analysed points are randomly distributed. (c) Carbon concentration of San Carlos olivine along a cross section. (d) Carbon distribution within melt inclusion of Silvestri olivine(1). Each concentration corresponding to one point is given in  $\mu\text{g/g}$ . Symbols are: shrinkage bubble, b; glass phase, gl; host olivine, ol.



**Figure 3.** Scapolite spectrum with two regions (C surface and C subsurface), 600 s. Charged particle spectra, same conditions as figure 1 except counting time.

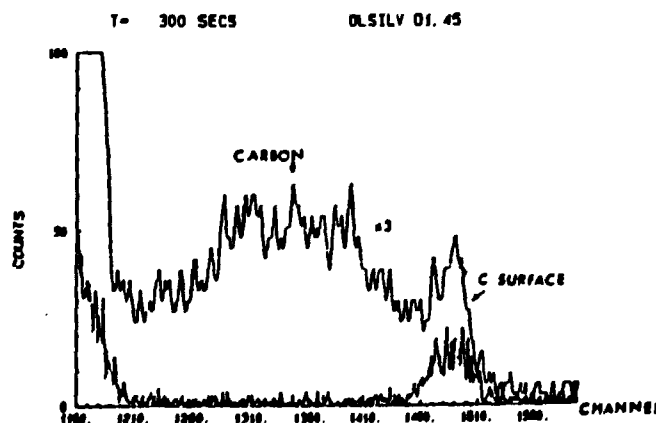


**Figure 4.** Spectrum from glass phase in Silvestri(1) (1892) sample, 300 s.

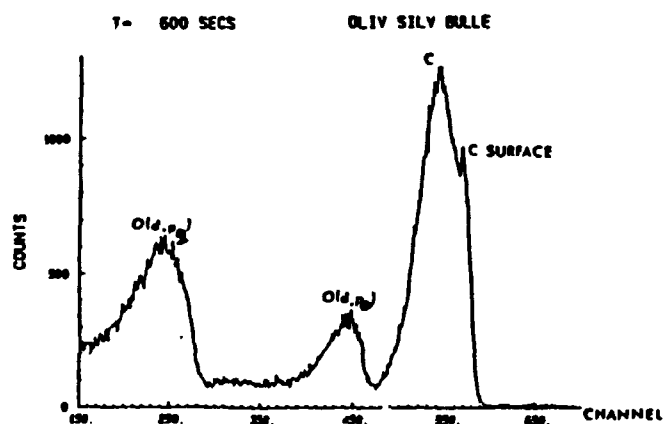


Figure 5. Spectrum from Silvestri shrinkage bubble (1) (1892) sample, 600 s.

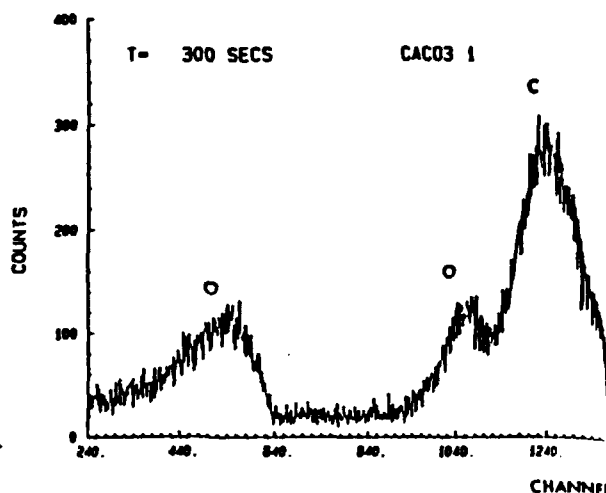


Figure 6. Calcite spectrum, 300 s. Bu) carbon target compared to thin carbon film of figure 5.

Charged particle spectra, same conditions as figure 1 except counting time.

### Results

A minimum detection limit (MDL) of 40  $\mu\text{g/g}$  was calculated from ALV 981 R23 basaltic fragments, with a 300-400 pA microbeam current intensity on the sample. On olivine crystals, 50  $\mu\text{g/g}$  is the lower detection limit because of Mg. For basaltic glass included in the olivine from Piton de la Fournaise, we obtain 60  $\mu\text{g/g}$  MDL (table 1) probably due to information loss due to the high current intensity (1200-1300 pA). We assumed a C content profile in the ALV 981 R23 sample. A higher content is present in  $\text{CO}_2$  gas bubbles in this material (they represent 1 to 5 vol.%), which decreases when one moves off (see table 1 and figure 2a). An average C content of 6000  $\mu\text{g/g}$  was calculated with the scapolite mineral (figure 2b). Seven points have been examined, exhibiting homogeneity on the surface and with depth as evidenced from the appearance of the spectrum (figure 3), which reproduces exactly the carbon C(d,p) excitation curve. For the olivine from San Carlos, two groups of values (table 1, figure 2c) show heterogeneities in the crystal. For the glasses trapped within Etnean minerals, we can take into account two types of heterogeneity (table 1, figure 2d). The data acquired for the glass phase (figure 4) and those for the shrinkage bubble infer a preferential concentration of carbon on the bubble walls (figure 5). The C spectrum corresponding to the melt inclusion bubble (figure 5), and a bulk target such as calcite (figure 6) were compared. The major difference is a C peak extension towards the lowest energies and, consistently, the existence of a superposition between C(d,p) and O(d,p) reactions, for the calcite spectrum (figure 6). So, the

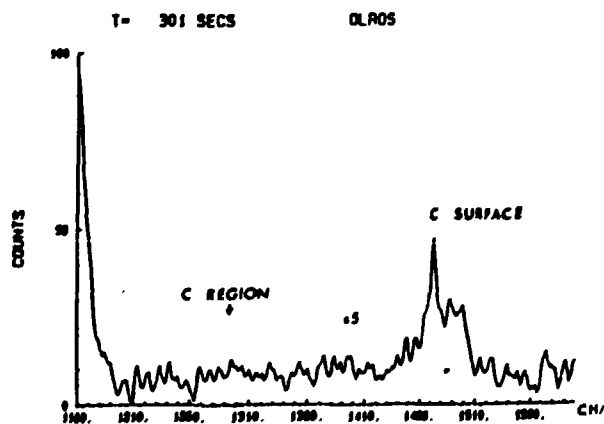


Figure 7. Charged particle spectrum from Mt. Rossi mineral sample. (Conditions figure 1 except  $t = 301$  s.)

thickness of the C film, on the bubble walls, could be estimated. It does not exceed 1 or 2  $\mu\text{m}$ . Also we found heterogeneities among the different melt inclusions examined. The concentrations vary from 70  $\mu\text{g/g}$  to 500  $\mu\text{g/g}$ . The C content of the host mineral (figure 7) is near the detection limit (50  $\mu\text{g/g}$ ). The observations and the results obtained from the Mt. Rossi and Mt. Silvestri samples are similar (table 1).

### Discussion and Conclusions

Our measurements may be compared to previously published data. The  $\text{CO}_2$  concentrations (2.5 wt%) of the scapolite from "La Chaine des Puys" correspond to the calculated values given by Boivin and Camus(7). These authors describe the difficulties in analyzing C in these kinds of minerals using classical methods. Our results point to an homogeneous distribution of this element within the selected sample.

The C content of Mg minerals such as olivine from San Carlos are lower than 100  $\mu\text{g/g}$ , close to the detection limit, neglecting the surface C. The measurements are reproducible and comparable to the bulk C content published for this material (5). Some anomalies were detected, inferring the existence of tiny  $\text{CO}_2$  rich inclusions. Measured concentrations and detection limit calculations are in accordance with previous data(10). Carbon contamination was limited to between 0 and 0.03  $\mu\text{m}$ .

For the glass fragment (ALV 981 R23), the C concentration obtained using mass spectrometry is 146  $\mu\text{g/g}$ (1). For the same specimens, lower values were found (95  $\mu\text{g/g}$ )(9) by infrared spectrometry. Our results lead to consideration of the existence of a concentration profile, between 1480  $\mu\text{g/g}$  to 100  $\mu\text{g/g}$ , with 425  $\mu\text{g/g}$  as the intermediate value. Undoubtedly, the highest content can be related to the existence of a  $\text{CO}_2$  gas bubble, previously described(9). However, some C determinations (around 250-500  $\mu\text{g/g}$ ) seem too high. Effectively, the C solubility is very low in basaltic liquids. For tholeiitic basalt outcropped on the sea floor (-2600 metres), published C concentrations range from 20 to 100  $\mu\text{g/g}$  (9). Other determinations for tholeiite lavas(1) indicate values between 141 to 171  $\mu\text{g/g}$ , under 250-275 bars  $\text{CO}_2$  pressure. Solubility of  $\text{CO}_2$  clearly depends on the pressure(1,7,9,11). If we consider 425  $\mu\text{g/g}$  C content as representative of the C dissolved in the tholeiitic liquid, the interpretation of the results is not easy. Similar data have been obtained on the glass inclusions trapped within Etnean phenocrysts.

We have examined the different parameters able to induce analytical errors, such as the beam current, the particle range calculations and the existence of other light elements as Li, B, F.

The current is monitored by use of the graphite standard. The composition of the different glass samples is similar, the stopping power in the matrix is also comparable, so this parameter cannot explain the observed variations. The other light elements (B, F, Li) could produce spectral interferences. However, their contents are low. For example, most fluorine determinations in basalts are lower than 500  $\mu\text{g/g}$ (12). We have not identified other characteristic peaks of those elements at upper energies. At this stage of our investigations, nothing permits us to assign to an experimental error the 400-500  $\mu\text{g/g}$  C contents measured on basaltic glass.

### Acknowledgement

This work was supported in part by the PIRPSEV (Programme interdisciplinaire de recherche sur la prévision et la surveillance des éruptions volcaniques).

### References

1. F. Pineau, M. Javoy, Earth Planet Sci. Letters, **62**, 239 (1983).

2. R. Clocchiatti, N. Metrich, *Bulletin Volcanologie*, 47, 3 (1985).
3. H. Bizouard et al., *Bulletin PIRPSEV*, 49 (1982).
4. F. Freund, *Contrib. Mineral. Petrol.*, 76, 474 (1981).
5. G. Oberheuser et al., *Geochim. Cosmochim. Acta.*, 47, 1117 (1983).
6. S. T. Tsong et al., *Phys. Chim. Minerals*, 12, 261 (1985).
7. P. Boivin, G. Camus, *Contrib. Mineral. Petrol.*, 77, 365 (1981).
8. Ch. Engelmann, J. Bardy, *Nucl. Instru. Methods in Phys. Res.*, 218, 209 (1983).
9. G. Fine, E. Stolper, *Earth Planet. Sci. Letters*, 76, 263 (1985/86).
10. E. A. Mathez et al., *Geophysical Research Letters*, 11, 947 (1984).
11. D. M. Harris, *Geochim. Cosmochim. Acta*, 45, 2023 (1981).
12. D. W. Muenow et al., *Earth Planet Sci. Letters*, 47, 272 (1980).